

Case Report

# Heavy Mineral Sands in Brazil: Deposits, Characteristics, and Extraction Potential of Selected Areas

Caroline C. Gonçalves and Paulo F. A. Braga \*

Centre for Mineral Technology (CETEM), Av. Pedro Calmon 900, Cidade Universitária, Rio de Janeiro 21941-908, Brazil; carolinec.gon@gmail.com

\* Correspondence: pbraga@cetem.gov.br; Tel.: +55-21-3865-7222

Received: 15 January 2019; Accepted: 6 March 2019; Published: 13 March 2019



**Abstract:** In Brazil, heavy mineral sand deposits are still barely exploited, despite some references to Brazilian reserves and ilmenite concentrate production. The goal of this project is to characterize and investigate the potential recovery of heavy minerals from selected Brazilian placer occurrences. Two areas of the coastal region were chosen, in Piauí state and in Bahia Provinces. In all samples, the heavy minerals of interest (ilmenite, monazite, rutile, and zircon) were identified by scanning electron microscopy (SEM) and X-ray diffraction (XRD) techniques and also quantified by X-ray fluorescence spectrometry (XRF) and Inductively Coupled Plasma Optical Emission Spectrometry (ICP-OES). The total heavy minerals (THM) in the Piauí samples were 6.45% and 10.14% THM, while the figure for the Bahia sample was 3.4% THM. The recovery test of the Bahia sample, using only physical separation equipment such as a shaking table and magnetic separator, showed valuable metallurgical recoveries at around or greater than 70% for each stage, and the final concentrate of pure ilmenite was composed of up to 60.0% titanium dioxide after the differential magnetic separation. Another aim is to compile accessible information about Brazilian heavy mineral main deposits complemented with a short economic overview.

**Keywords:** heavy mineral sands; Brazilian occurrences; SEM analysis; XRF analysis

## 1. Introduction

Although Brazil is considered the biggest producer of titanium dioxide in Latin America [1,2], mostly from ilmenite, studies about heavy minerals in the national territory are still scarce, limiting exploration works. The constant reference to heavy minerals such as ilmenite, zircon, and rutile as byproducts of rare earth element (REE) deposits, reveals the lack of information or a consolidated database about Brazilian heavy mineral sand deposits. The mention of defunct institutions as producers, and inaccurate grade-tonnage calculations of heavy mineral sands in international publications are common mistakes due to dispersed and hard-to-access information. Research aiming to identify new target areas and to compile accessible data seems to be a necessary step to plan future projects, considering the relevance of heavy mineral deposits in the international market.

In fact, heavy mineral sands are different than other commodities in terms of exploration, development, mining, and processing, but similar in the matter of importance to industry due to their relevant physical properties [3]. Heavy mineral sand deposits are generally voluminous and near to the surface, facilitating simple exploration techniques and open cast excavation [4]. Moreover, heavy mineral processing plants are currently well-established and highly mechanized, with considerable separation efficiency [4]. Usually, heavy minerals from beach sands are concentrated by physical methods, first involving gravity separation, followed by the combination of magnetic and electrostatic

separation [5–8]. Flotation is also used [9,10], often as a subsequent and/or complementary stage, in an effort to achieve a cleaner product [11].

Globally, the leading producer of heavy minerals is Australia followed by South Africa [12]. The massive Australian participation in the international market has been consolidated since the 1960s [11]. Furthermore, according to Gosen et al. (2016) [4], China had the biggest production of ilmenite concentrate in 2014. In Brazil, however, the deposits of heavy mineral sands are largely not exploited, with the only active operation being the Guaju mine (Cristal Group) located in Paraíba Province. The main minerals processed from that mine are ilmenite, rutile, zircon, and kyanite. Likewise, the company Industrias Nucleares do Brasil (INB), in Rio de Janeiro Province, still produces ilmenite, zircon, rutile, and monazite concentrates for sale as is.

The importance of coastal heavy mineral deposits as sources of rutile, ilmenite, and zircon for industry, and their worldwide uses, have always been mentioned [13]. These deposits are a source of titanium and zirconium [4] as well as rare earth elements (REEs), and are often overlooked [14]. In Brazil, some found occurrences of monazite and its secondary products (ilmenite, zircon, and rutile) are along the coastline [15,16], and most studies have been specifically developed to find REE deposits (Figure 1). Practically all of them are located in the southeast region as described in Louwerse (2016) [17].

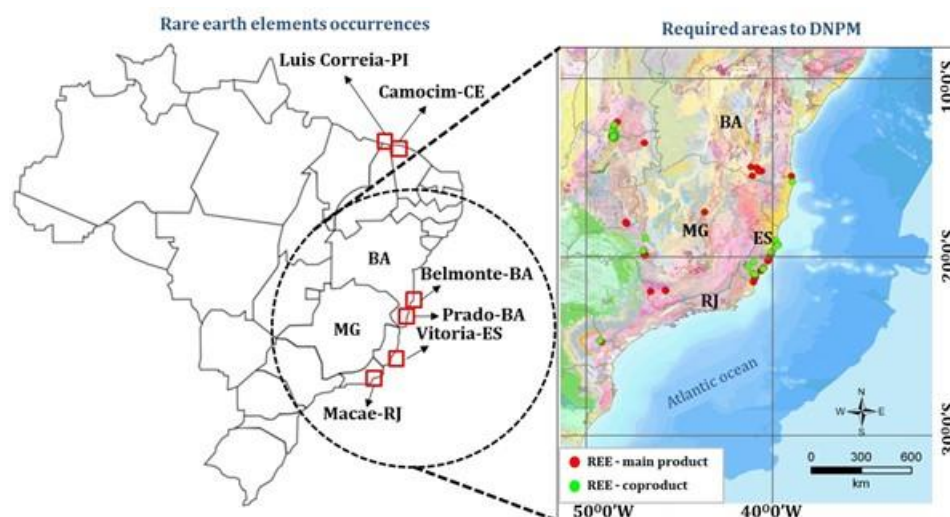


**Figure 1.** Rare earth elements (REEs)-bearing mineral occurrences along the Brazilian coastline and areas licensed by the National Department of Mineral Production (DNPM) for extraction of REEs. Adapted from [15,16].

As cited by CETEM (2014) [18], the presence of surface and submerged deposits of ilmenite, rutile, zircon, and monazite is along nearly the entire Brazilian littoral, from Para to Rio Grande do Sul. In these regions, including the northern portion, other profitable placer deposits of heavy mineral sands are/were being exploited, like in Sao Francisco de Itabapoana (Rio de Janeiro), Mataraca (Paraíba), and Prado (Bahia). However, according to Krishnamurthy and Gupta (2016) [19], mineral sand mining in Brazil is oriented to the thorium content of monazite, in contrast with other countries, where monazite is a secondary product rather than ilmenite, rutile, and zircon. In fact, in the past, exploration efforts for finding monazite deposits were connected with the intention of producing REE oxides for nuclear purposes [18]. INB for instance, which has mined and processed heavy minerals in the northern coastal region of Rio de Janeiro, is recognized for its monazite sand deposits. The Heavy Minerals Unit of Buena is the most relevant plant for monazite concentration, but has been decommissioned. Nowadays, monazite concentrates come from old mining activities and will likely be produced for two or three more years.

The production of titanium dioxide in Brazil started in 1971, and at present, heavy minerals such as ilmenite, rutile, kyanite, and zircon [20,21] are extracted at the Guaju mine [5] by the Cristal Group. The presence of monazite is also well known on the deposit [22,23]. Nevertheless, their reserves may be exhausted within a few years. Currently, some efforts for an independent national production of titanium mineral concentrates have been made by Rio Grande Mineração S. A., based on a forecast for growth of the Brazilian ilmenite consumption. They estimate an annual production of 323,000 tons of heavy mineral concentrates, 275,000 being ilmenite, 10,000 rutile, and 38,000 zircon [24].

A comparison of Brazilian heavy mineral resources and production with other countries is given every year by the National Department of Mineral Production (DNPM) [1]. Data compilation from 2009 to 2015 for ilmenite, rutile, and zircon are shown in Figure 2. Although Brazil has modest resources and production of zircon concentrate, in the national market of heavy mineral sands, ilmenite and rutile concentrates are considered the main products. Indeed, in more recent data [25], Brazilian ilmenite resources are still considered small, only about 5.6% of global resources. As described in Technical Report 36 [26], Brazilian production of titanium concentrates (ilmenite plus rutile) has oscillated considerably, with the most relevant decline since 1986 occurring in 2001, when production was only 64,450 tons. The highest titanium production, however, was in 2007 with 226,865 tons, and in 2015, the most recent data, was 81,000 tons [1].

Furthermore, the production of zircon, from 2003 to 2015, varied from 16,000 to 28,000 tons per year and the assigned resources decreased from 74 Mt in 2009 to approximately 22,6000 tons in 2015 (Figure 2). Placer deposits are considered the secondary source of zircon in Brazil, since primary sources are those related with intrusive alkaline rocks [1]. The monazite resources and production data are always included as one of the sources of REEs and their specific quantification is more complex. The preliminary calculated Brazilian monazite resources are 22 Mt [1]. The production of monazite concentrates, however, has significantly oscillated, falling from 1,173 tons in 2007 to 249 tons in 2010. More recent data showed a production of 600 tons in 2013 and no production in 2015 [1]. Although this was a small production, all monazite concentrate produced by INB in this period from 2003 to 2015 was exported [1].

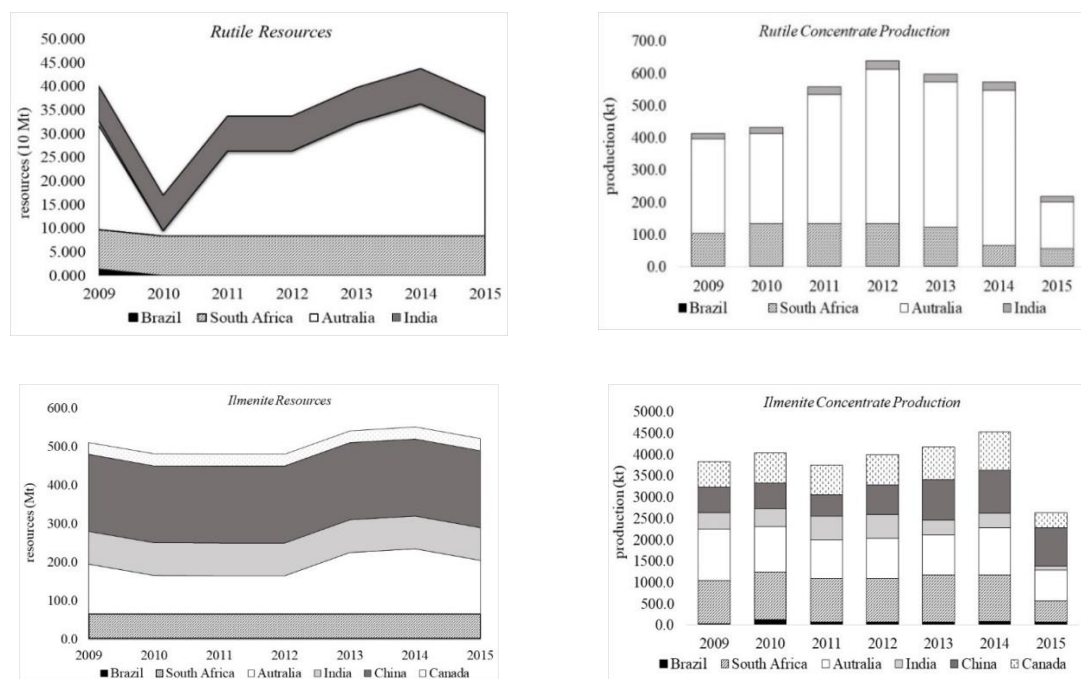
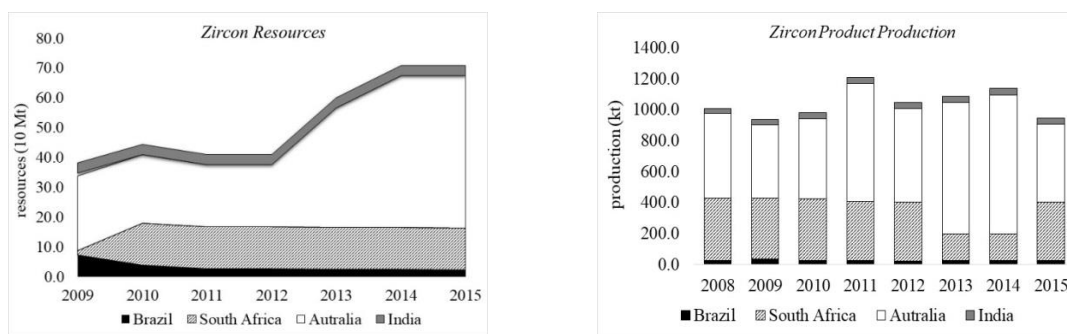


Figure 2. Cont.



**Figure 2.** Brazilian resources and the production of ilmenite, rutile, and zircon concentrates, in comparison with the main global producers. Compiled from [1].

Therefore, a project for the characterization and recovery of heavy minerals from selected Brazilian placer occurrences was developed. The study was aimed at compiling accessible information about the main Brazilian deposits of heavy mineral sands [15,16,27–32], complemented by a short economic overview, highlighting the presence of ilmenite, zircon, monazite, and rutile. Two areas of the Brazilian coastal region were chosen for characterization studies.

## 2. Study of Potential Areas

### 2.1. Sampling Areas

Two potential areas were chosen based on previous studies [27,30] and recent exploration works [31]. These areas are located in Luis Correia/Piauí and Prado/Bahia. Three samples have been collected, two of them in Luis Correia (LC and LP) and one in Prado (PA) (Figure 3). In Luis Correia, the samples were collected by the grab sample technique, and due to a limited amount of collected material (at around 9.0 kg for each sample) and the lack of representativeness, LC and LP samples were characterized just in order to identify potential heavy minerals for future works. Conversely, around 0.5 tons of heavy mineral sands were collected in Prado (PA sample) by the trenching sampling method (at around 1.5 m depth). The spot was chosen supported by the local company's geochemical studies. The PA sample was also subjected to recovery tests.

The presence of heavy minerals in Luis Correia region was confirmed in the 1980s when the Samitre Company surveyed this occurrence and classified it as a medium deposit, with resources of approximately 1,500,000 tons [30]. According to the Brazilian Mineral Resources Company (2014) [29], Luis Correia district is classified as coastal deposits with fine sand. Moving dunes (Figure 3a,b) and paleodunes are composed mainly of selected quartz or quartz-feldspar sediments formed during the Quaternary Period [28].

Prado is also characterized by an accumulation of sediments of the Quaternary Period. Conversely, other authors [27] mentioned that the geological context of this area may be described by an accumulation of sediments from the Cretaceous to the Tertiary Periods associated with Archean rocks, which could have been a source of heavy minerals. Additionally, north Prado is in direct contact with Barreiras Group where sediments are classified as well as selected coarse sand (Figure 3c) [29]. About heavy mineral occurrences, Louwse (2016) [17] cited that Prado region has monazite resources (approximately 4,464 tons) composed of 19.98% REE oxides, including the presence of xenotime and allanite minerals [17]. In fact, Cumuruxatiba and Alcobaca, near to Prado, have been sources of heavy minerals since the 18th century when monazite was sent to Europe [27].

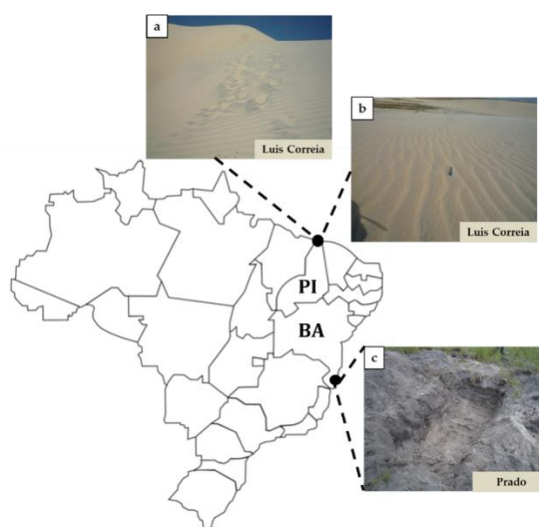


**Figure 3.** Sampled areas: LP (a), LC (b), and PA (c).

## 2.2. Analytical Tools and Methods

Samples were characterized in three main parts: (1) the raw material; (2) sink dried aliquots separated by methylene iodide ( $d = 3.32 \text{ g}\cdot\text{cm}^{-3}$ ) as a heavy medium and by a Frantz Isodynamic Separator (Model L-1, S.G. Frantz Co., Moorestown, NJ, USA) (transverse slope  $\theta$  set at  $15^\circ$ ), and (3) products and tailings recovered from test steps. Techniques and equipment are: optical microscopy, chemical analysis by X-ray fluorescence spectrometry (XRF, Axios Max Rh emission spectrometer, Malvern Panalytical Ltd., Royston, UK) and by inductively coupled plasma optical emission spectrometry (ICP-OES, Ultima 2 spectrometer, HORIBA Instruments Brasil, Ltda., Sao Paulo, Brazil); mineralogical analysis by X-ray diffraction (XRD, AXS D4 Endeavor co-emission diffractometer, Bruker, Karlsruhe, Germany) and by scanning electron microscopy (SEM, TM 3030 Plus tabletop microscope, Hitachi, Tokyo, Japan) with energy dispersive X-ray analysis (EDX); and density measurements by pycnometry (AccuPyc II 1340, Micromeritics, Norcross, GA, USA) with helium as analyzing gas. It is important to note that for XRF and XRD analysis, all samples tested were homogenized in longitudinal piles, and then quartered using a rotating laboratory sample divider. For XRD, representative aliquots of 3 g of each sample were ground with 10 mL of deionized water using a McCrone mill (Microne micronising mill, Glen Creston, Westmont, CA, USA) for 10 min, and after dried. For XRF, representative aliquots of 30 g were ground using a laboratory pulverizer (carbide ball mill, pulverisette, Fritsch, Idar-Olberstein, Germany) and then separated into 5 g aliquots using the same rotating laboratory sample divider.

## 2.3. Recovery Test

A pilot plant test using gravity and magnetic separation methods (Figure 4a) was performed on a 28.7 kg PA sample. Before all tests, a wet cleaning stage was carried out due to a great amount of organic material, which was partially responsible for the dark color (Figure 3c). The cleaned sample still had 3.0% of organic material measured in terms of loss on ignition (LOI) using a TGA-701 Thermogravimetric Analyzer (LECO Instrumentos Ltda., Rio de Janeiro, Brazil). Then, the cleaned sample was wet screened using a 297  $\mu\text{m}$  aperture and the undersize (pulp with 35% solids) sent to a Super Duty Diagonal Deck shaking table (slope set at  $10^\circ$ ). Furthermore, the heavy fraction was separated in an Inbras high intensity magnetic separator with a magnetic field strength of 4.5 T (Tesla). However, the nonmagnetic concentrate had to be separated again from light minerals by using a shaking table. In addition, the magnetic concentrate (about 800.0 g) was wet screened using a 212  $\mu\text{m}$  aperture, and then each aliquot (oversize and undersize) was separated at the same Inbras high intensity magnetic separator, changing its belt speed (Figure 4b). The belt speed was adjusted to

50 rpm (rotations per minute) for each test, reaching 300 rpm maximum. Due to a higher magnetic susceptibility, minerals such as ilmenite should be recovered at the highest belt speed.

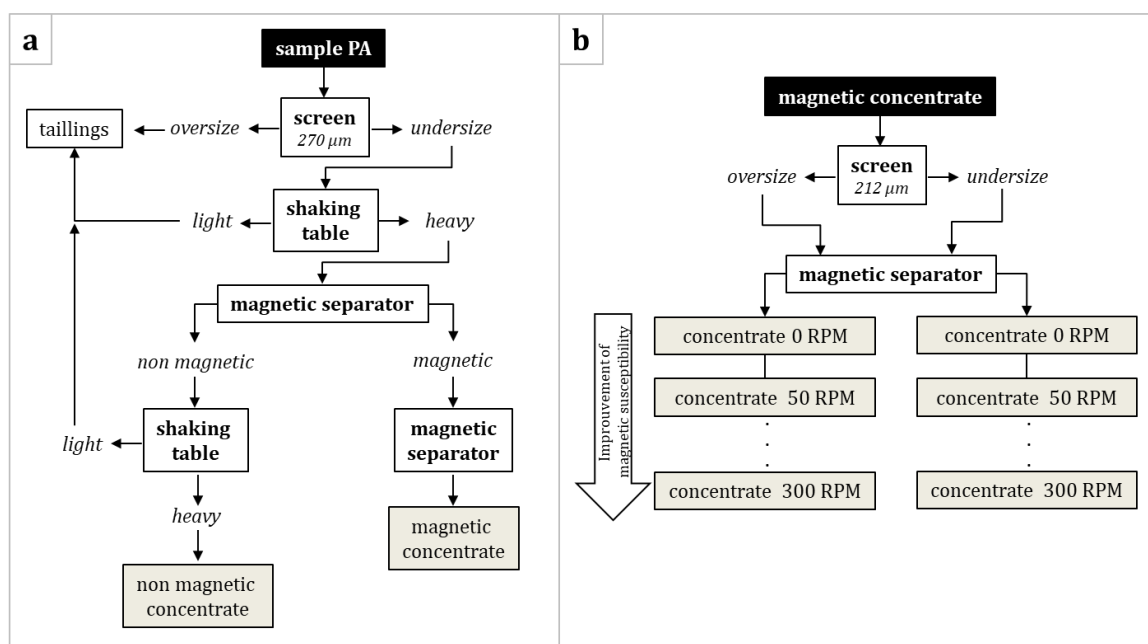


Figure 4. Main recovery test flow sheet (a) and differential magnetic separation flow sheet (b).

### 3. Results and Discussion

#### 3.1. Characterization and Identification of Heavy Minerals

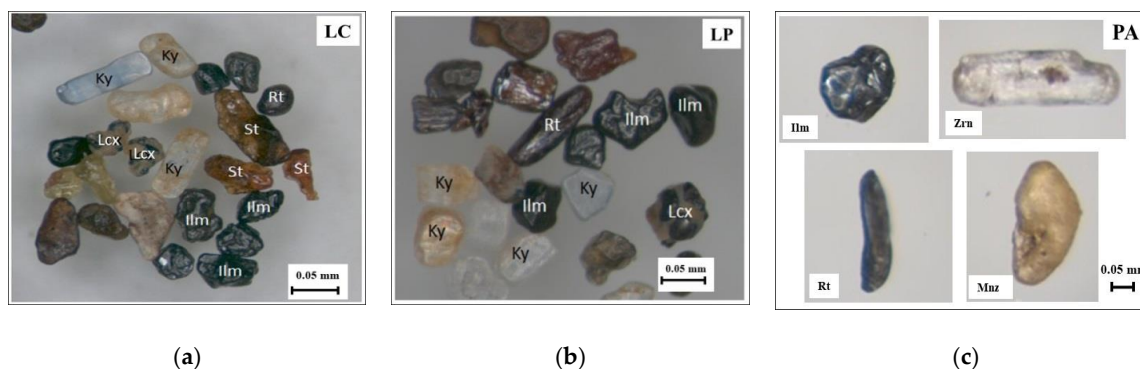
The samples' physical properties are given in Table 1. Specifically in this study, in order to facilitate characterization works, avoiding excessive contamination by silicates, total heavy mineral quantification was done using methylene iodide. Consequently, all minerals which have a density higher than  $3.32 \text{ g}\cdot\text{cm}^{-3}$  were considered as heavy minerals (THM). Those heavier than  $3.32 \text{ g}\cdot\text{cm}^{-3}$ , which were recovered up to 1.3 T magnetic field strength by a Frantz Isodynamic Separator, were also considered as total magnetic heavy minerals.

Table 1. Classification of the three samples.

Property	LC	LP	PA
Total heavy minerals (THM) (%)	6.45	10.14	3.40
Total magnetic heavy minerals (%)	65.60	64.40	94.12
$d_{80}$ passing size ( $\mu\text{m}$ )	190	400	730
Slimes ( $-45 \mu\text{m}$ ) (%)	0.31	0.11	0.10

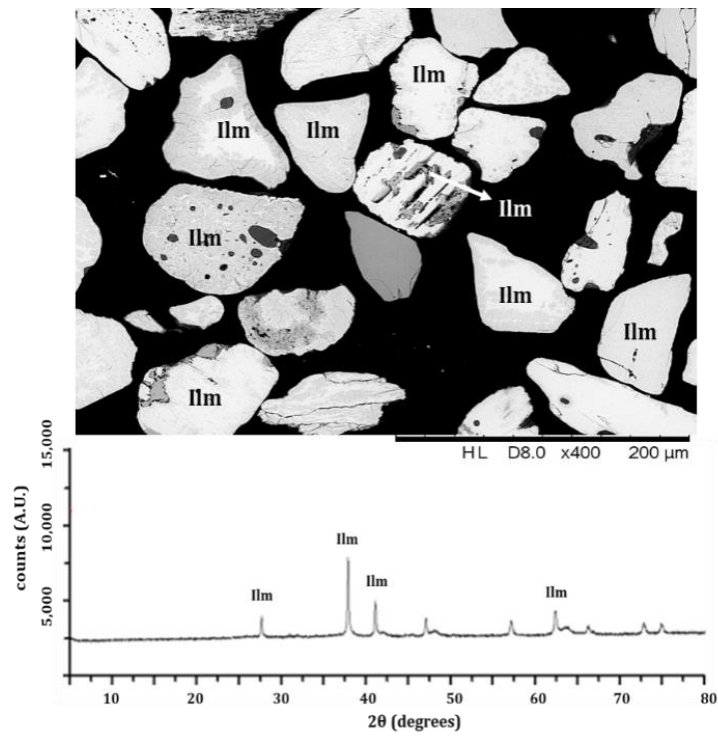
Based on the characterization analysis, both areas show the four minerals of interest, i.e., monazite (Mnz), rutile (Rt), zircon (Zrn), and ilmenite (Ilm), the latter mineral being the most abundant. Additionally, XRD and Rietveld quantification were performed. Using the software Bruker AXS Topas, (version 5), the phases were quantified. Their crystalline structures were identified using the following databases: Bruker AXS, Inorganic Crystal Structure Database (ICSD) [33], and Crystallographic Open Database (COD) [34]; refining variables were adjusted to those corresponding to the equipment standard. The result for the raw material demonstrated 0.7% ilmenite, 0.2% monazite, 0.3% rutile, and 0.2% zircon for LC; the LP sample was composed of 4.4% ilmenite, 1.6% monazite, 0.4% rutile, and 1.3% zircon. These two samples were also composed of minerals such as actinolite, epidote, muscovite, kyanite (Ky), staurolite (St), and leucoxene (Lcx). Details of some identified minerals from LP and LC

are given in Figure 5. Due to the proximity of the sampled points, their mineralogical assemblages are quite similar. However, for the PA sample, although the Rietveld method allows the quantification of the amount of amorphous minerals [35], the results were not precise especially for minor minerals such as monazite and rutile due to the great presence of light minerals (higher than 96% in terms of mass distribution), and consequently, XRD interpretations were not considered.

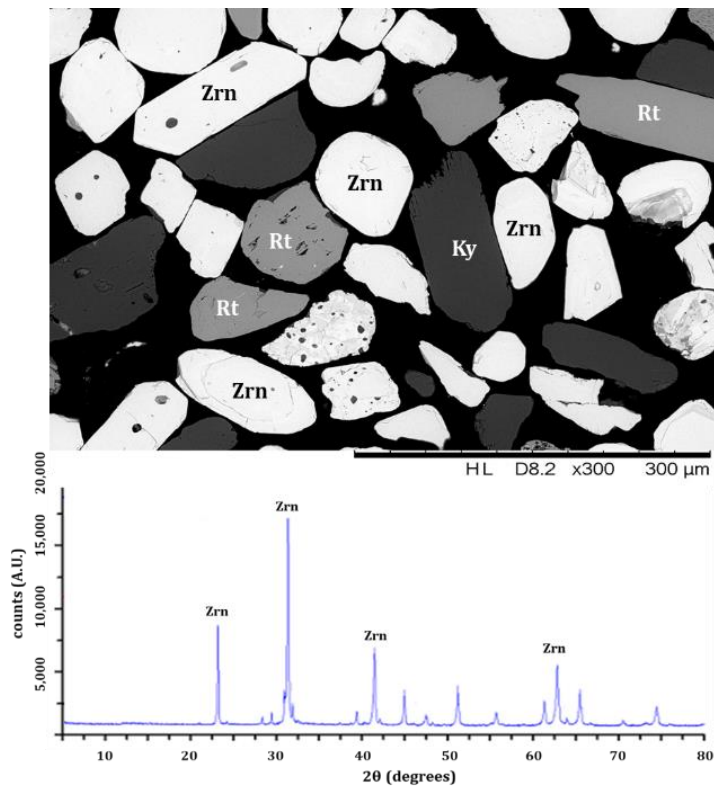


**Figure 5.** Examples of some heavy minerals identified via optical microscopy of LC (a), LP (b) and PA (c) samples. Note: Ilm: ilmenite, Ky: kyanite, Lcx: leucoxene, Mnz: monazite, Rt: rutile, St: staurolite and Zrn: zircon.

The separation by a heavy medium (methylene iodide) followed by a separation using a Frantz Isodynamic Separator allowed a better observation of those heavy minerals present in the samples. This stage provided important information about mineral alterations and inclusions, which can determine further beneficiation tests. An average of 65% by weight of LC and LP sink fractions were composed of magnetic heavy minerals. Ilmenite (Ilm) was the most abundant mineral in both samples and concentrated at 0.450 T fraction (Figure 6a); magnetite was also detected in this fraction. The ilmenite grains are extremely altered sometimes in pseudorutile and anatase (grain boundaries), as reported by [36], and also leucoxene (Figure 5a,b). These ilmenite grains showed selective alteration (Figure 6a) as well. The boundary alterations might be due to the reducing conditions of the geological environment [37]. However, although these alterations did not affect ilmenite recovery at the theoretical magnetic field strength at 0.450 T, ilmenite was also retained at 0.675 T. Ilmenite was usually found in pure form but a minor presence of manganese (Mn) has also been observed by EDX for both Luis Correia samples. Minerals such as monazite, stautolite, actinolite, and amphiboles were founded at 0.950 T fraction. In addition, the nonmagnetic fraction contains mostly prismatic and rounded zircon (Zrn) with kyanite (Ky) inclusions, and rounded and prismatic rutile (Rt) (Figure 6b). Despite the fact that zircon composition is not comparable to the theoretical due to the presence of niobium (Nb) and aluminum (Al), the hafnium (Hf) and zirconium (Zr) ratio are 0.04 for both samples as described elsewhere [38]. Al-silicates such as kyanite present in the nonmagnetic fractions of LC sample, for instance, are coarser than 74  $\mu\text{m}$ , facilitating their separation by size from zircon; in other deposits this separation is more complicated [38] and a flotation stage is needed [10].



(a)



(b)

**Figure 6.** SEM images of LC heavy minerals retained at 0.450 T (a) and the nonmagnetic fraction (b) separated by a Frantz magnetic separator and their respective XRD spectra showing the main mineral of the fraction.

SEM image mapping of PA by element (Ti, P, Fe, Zr, and Si) of the sink fraction is shown below (Figure 7a). This image confirms the high presence of ilmenite rather than other heavy minerals such as zircon and monazite. In this analysis, no rutile was found. Monazite (Figure 7b) is the main mineral retained at 1.3 T and according to EDX data composed of REE Ce (24.4%), La (15.9%), Nd (6.1%), and Th (7.9%) on average. Monazite grain shapes are very variable and can vary from elongated to subrounded. In addition, in the nonmagnetic fraction, minerals such as zircon and rutile are mainly composed of 38.0% ZrO<sub>2</sub> and 53.1% SiO<sub>2</sub>, and 89.3% TiO<sub>2</sub>, respectively.

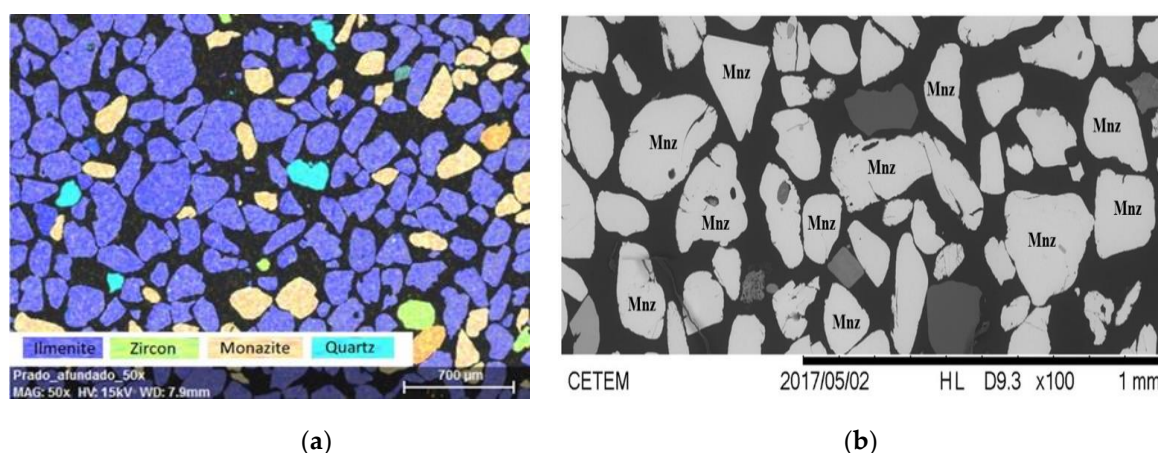


**Figure 7.** SEM image mapping of PA sink fraction (a) and SEM image of sink fraction retained at 1.3 T (b).

In PA heavy minerals retained at 0.675 T, it is possible to observe the presence of ilmenite, some zircon (inclusions), monazite, and xenotime. Although the latter is not abundant, it is also an interesting mineral since yttrium (Y) is an REE. According to EDX, its composition is 38.52% O, 37.34% Y, 22.96% P, and 1.17% Al. Ilmenite is the most abundant mineral in this fraction and is altered into anatase, especially along its boundaries and fractures (Figure 8a). Not just along its boundaries and fractures but EDX results showed that PA ilmenite might be considered an altered ilmenite since its Ti content is higher (34.85%) than the theoretical value (31.56%) [39]. Additionally, this Ti increase is observed followed by a decrease in the Fe percentage as suggested by Temple (1966) [40]. Another fact about PA ilmenite is the negligible amount of Mn in its composition. Nevertheless, this element was not quantified by EDX, the small Mn peak close to 6.0 keV [41] can still be observed (Figure 8a). Some Fe remains in the composition of the ilmenite alteration, as can be seen in Figure 8b.

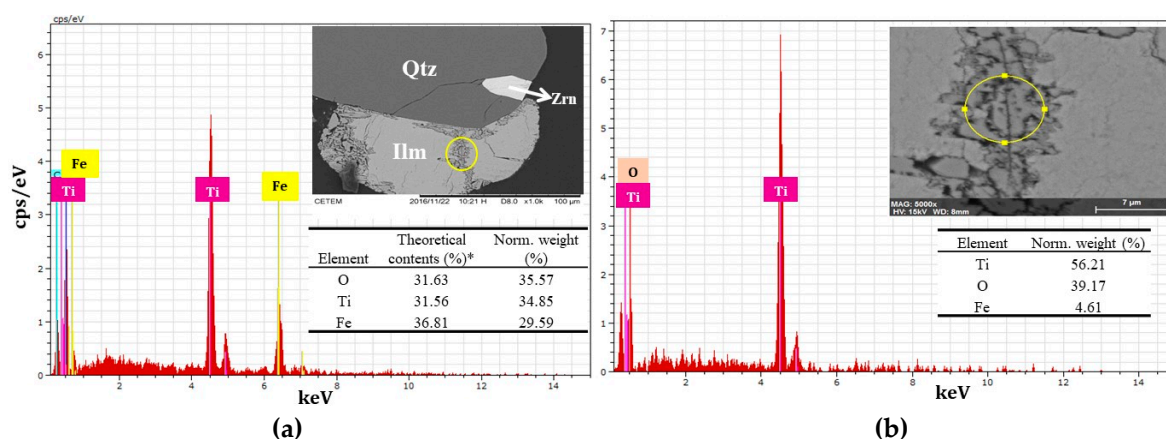


**Figure 8.** SEM images and EDX results for ilmenite (a) and details of its alteration (b). \* Note: values from Dana (1974) [39].

Chemical analysis was also carried out. The head assay results of the oxides of interest are shown in Table 2. For PA, due to the low content of REEs ( $\text{CeO}_2$ ,  $\text{La}_2\text{O}_3$ , and  $\text{Nd}_2\text{O}_3$ ), thorium (Th), and zirconium (Zr), the chemical analysis by ICP-OES was carried out, showing 603.19 ppm of  $\text{CeO}_2$ , 570.91 ppm of  $\text{La}_2\text{O}_3$ , 450.42 ppm of  $\text{Nd}_2\text{O}_3$ , 107.51 ppm of  $\text{ThO}_2$ , and 456.77 ppm of  $\text{ZrO}_2$ .

**Table 2.** Selected major elements of whole rock sample according to X-ray fluorescence spectrometry (XRF) results.

Sample	$\text{Fe}_2\text{O}_3$ (%)	$\text{TiO}_2$ (%)	$\text{ZrO}_2$ (%)	REE + $\text{P}_2\text{O}_5$ (%)
LC	1.4	1.5	0.36	<0.1
LP	2.2	2.6	1.1	0.2
PA	0.7	1.5	<0.1	<0.1

Note: REE ( $\text{CeO}_2$ ,  $\text{La}_2\text{O}_3$ ,  $\text{Nd}_2\text{O}_3$  +  $\text{ThO}_2$ ).

Overall, it was possible to observe a significant difference between the Luis Correia samples and the Prado sample (Figure 9) in terms of in which particle size interval the oxides of interest ( $\text{TiO}_2$ ,  $\text{ZnO}_2$ ,  $\text{Fe}_2\text{O}_3$ , REE oxides, and  $\text{P}_2\text{O}_5$ ) are. These oxides are preferentially concentrated at  $-150 +53 \mu\text{m}$  for LC (Figure 9a), at  $-106 +53 \mu\text{m}$  for LP (Figure 9b), and for PA at  $-297 +106 \mu\text{m}$  size fractions (Figure 9c). Specifically about PA REE oxides +  $\text{P}_2\text{O}_5$ , they tend to concentrate at  $-297 +150 \mu\text{m}$ , where almost 28.6% of the total mass contained 83.4% of the REE oxides and  $\text{P}_2\text{O}_5$ . Moreover, in LC, 31.39%  $\text{P}_2\text{O}_5$  content is concentrated at  $-75 +53 \mu\text{m}$  and for LP this value is 46.57%, in terms of mass distribution.

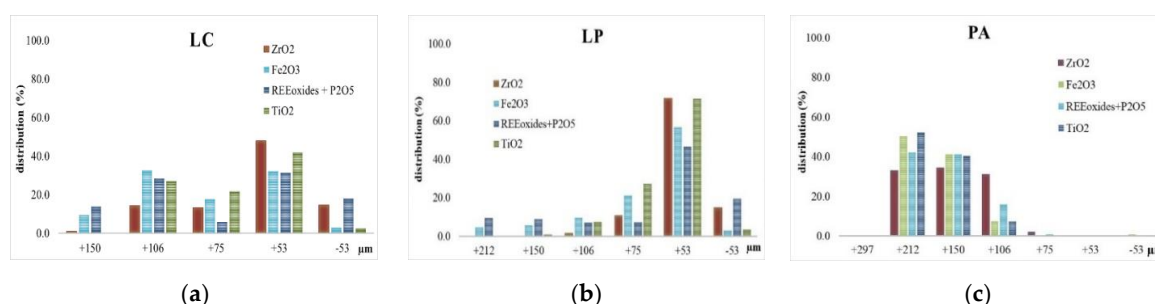


**Figure 9.** Selected major elements in terms of oxides ( $\text{ZrO}_2$ ,  $\text{Fe}_2\text{O}_3$ , REE+ $\text{P}_2\text{O}_5$  and  $\text{TiO}_2$ ) of raw material by size fraction of LC (a), LP (b) and PA (c) samples, according to the XRF results.

### 3.2. Recovery Test of Bahia Sample

Mass and metallurgical balances of the recovery test are presented in Figure 10 as well as the particle distribution of the tested sample. The oxides considered for the process control were  $\text{SiO}_2$  for quartz and other light minerals,  $\text{TiO}_2$  for ilmenite and rutile,  $\text{ZrO}_2$  for zircon, and  $\text{P}_2\text{O}_5$  for monazite. The  $\text{SiO}_2$  present in the zircon structure was discounted based on the average of the EDX values.

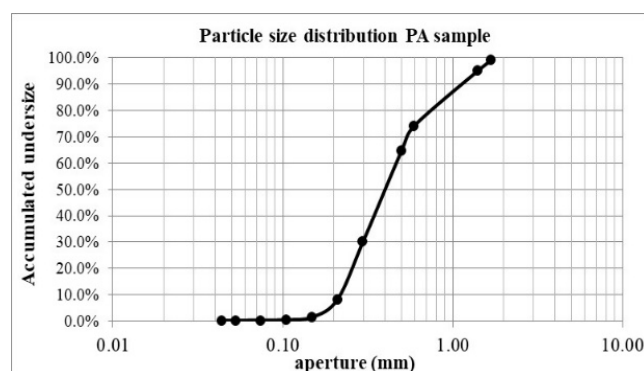


**Figure 10.** Cont.

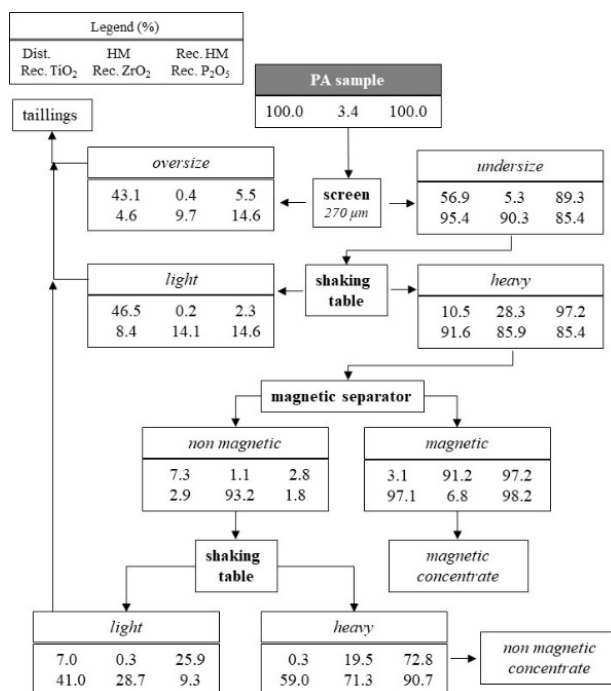


**Figure 10.** Particle size distribution of the PA sample (a) and mass and metallurgical balances (b).

The first gravity separation by shaking table shows values up to 85.0% for metallurgical recoveries of TiO<sub>2</sub>, ZrO<sub>2</sub>, and P<sub>2</sub>O<sub>5</sub>. The percentage of heavy minerals rises from 3.4% to 28.3%. After the magnetic separation stage, two bulk concentrates are obtained. Zircon is concentrated in the nonmagnetic concentrate, where 93.2% ZrO<sub>2</sub> is recovered. However, this fraction was still very contaminated with quartz (96.8% SiO<sub>2</sub> content due to quartz and other light minerals). Because of that, an additional shaking table cleaning stage was added in the process, obtaining a final nonmagnetic concentrate with 19.5% heavy minerals. This concentrate has 7.7% ZrO<sub>2</sub> with good ZrO<sub>2</sub> recovery (71.3%). Presumably, the titanium-bearing minerals such as rutile (Figure 5) are also in the nonmagnetic fraction due to its TiO<sub>2</sub> content (6.6%).

The magnetic concentrate is composed of 50.5% TiO<sub>2</sub> and 2.5% P<sub>2</sub>O<sub>5</sub>, and for the individualization of ilmenite and monazite, a differential magnetic separation was used, which related the distinct mineral magnetic susceptibilities with the belt speed of the magnetic separator (Figure 11). In this process, 0 rpm is a reference to nonmagnetic minerals still present in the magnetic concentrate (11.1% SiO<sub>2</sub> and 0.2% ZrO<sub>2</sub>). The fractions tested were −270 μm, +212 μm, and −212 μm. The variations of fraction densities according to the belt speed are described in Figure 11a. These values were compared with theoretical densities of ilmenite (4.7 g·cm<sup>−3</sup>), monazite (5.0 to 5.3 g·cm<sup>−3</sup>) and quartz (2.65 g·cm<sup>−3</sup>) [39]. Thus, it is possible to infer that monazite was concentrated at 150 rpm for the −212 μm fraction and at 200 rpm for the +212 μm fraction, whereas ilmenite was recovered at 100, 150, and up to 200 rpm for the +212 μm fraction, and at 150 rpm and up to 200 rpm for the −212 μm fraction. Consequently, the finer material (−212 μm fraction) has more minerals with low magnetic susceptibility, namely monazite, which is in accordance with Figure 9. The ilmenite final concentrate is considered that recovered at 250 and 300 rpm, and according to the chemical analysis by XRF (Figure 11b), TiO<sub>2</sub> content is slightly higher than 60.0%. This value is consistent with those found for the composition of PA ilmenite, suggesting the presence of altered ilmenite with a lower Fe content and higher Ti content, as verified in the characterization studies (Figure 8a). The P<sub>2</sub>O<sub>5</sub> content reaches values of almost 20.0% at 150 rpm for the −212 μm fraction, while for the same belt speed the content was 10.0% for the coarser fraction (+212 μm) (Figure 11b). Overall, in both size fractions, SiO<sub>2</sub> content decline significantly (less than 5.0% in each material recovered from 50 to 300 rpm) and the

average  $ZrO_2$  content is 0.66% at 0 rpm. This result demonstrated the possibility of selective separation between ilmenite and monazite by varying the belt speed of the magnetic separator.

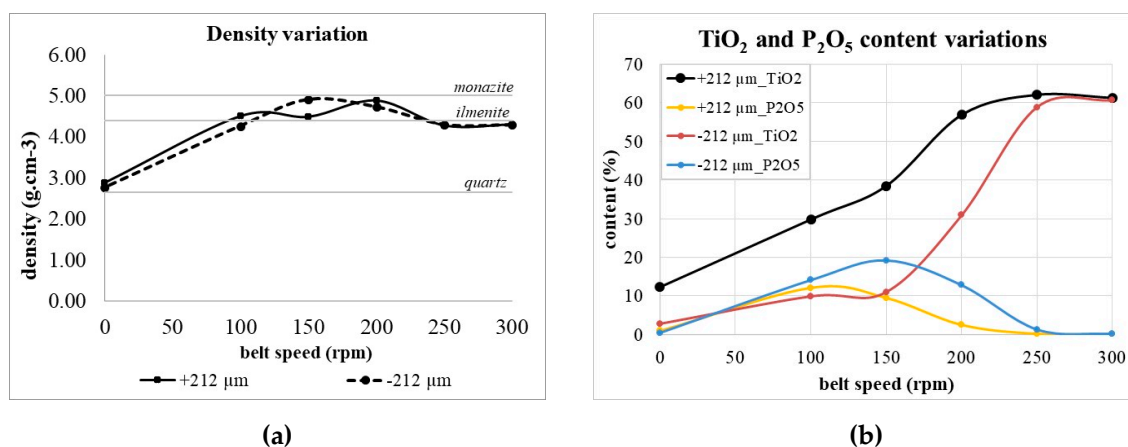


**Figure 11.** Density variations of the material recovered in different belt speeds (a), and variation of selected oxide ( $TiO_2$  and  $P_2O_5$ ) contents for +212  $\mu m$  and  $-212 \mu m$  size fractions according to the magnetic separator's belt speeds (b).

#### 4. Conclusions

This study shows a compilation of data of Brazilian heavy mineral sands. The Brazilian deposits of heavy minerals have been known since the 1940s, with the beginning of monazite concentrate production by INB. Some of these deposits are located along the southeast Brazilian coastline, especially in Rio de Janeiro and Espirito Santo Provinces. However, they are not widely explored, being restricted nowadays to the Brazilian northern region at Guaju mine (Cristal Group) in Paraiba Province, where the reserves may be exhausted within a few years. Only one new project, to extract ilmenite in Sao José do Norte, Rio Grande do Sul Province, was found.

The other question is that the constant reference to heavy minerals such as ilmenite, zircon, and rutile as byproducts of REE deposits gives the impression of a lack of information or a consolidated database in their respect. Normally these sources are restricted to private companies or dispersed among public entities. Despite the existence of references to Brazilian resources in many reports around the world, investments in this sector are low.

In the two studied areas (Piauí and Bahia), the heavy minerals of interest (ilmenite, monazite, rutile, and zircon) were identified by SEM and XRD analyses. The total heavy minerals of the two Piauí samples, LC and LP, were 6.45% and 10.14%, respectively, and for the Bahia sample, the figure was 3.4%. The head assays of the main oxides, by XRF, showed contents of 1.5%, 2.6%, and 1.5% of  $TiO_2$  for the LC, LP, and PA samples. LP had the highest content of  $ZrO_2$  (1.1%) and REEs ( $CeO_2$ ,  $La_2O_3$ ,  $Nd_2O_3$ , and  $ThO_2$ ), and  $P_2O_5$  (0.2%). For PA, due to the low contents of REEs, thorium (Th), and zirconium (Zr), chemical analysis by ICP-OES was carried out, showing 603.19 ppm of  $CeO_2$ , 570.91 ppm of  $La_2O_3$ , 450.42 ppm of  $Nd_2O_3$ , 107.51 ppm of  $ThO_2$ , and 456.77 ppm of  $ZrO_2$ . However, the THM of these occurrences is still quite low when compared with other deposits, and just reinforces the small Brazilian participation in this market (Figure 2). Investments in exploration works for heavy mineral sands could change this scenario.

The recovery test of the Bahia sample, using physical separation equipment such as a shaking table and a magnetic separator, showed valuable metallurgical recoveries at around or greater than 70% for each stage (Figure 10), demonstrating a reliable test execution. The final concentrate of ilmenite is composed of up to 60.0% titanium dioxide after differential magnetic separation. These concentrates obtained for +212  $\mu m$  at 250 and 350 rpm, and  $-212 \mu m$  at 300 rpm could even be commercialized since their contents satisfy specifications of the Brazilian market (53%  $TiO_2$  and  $<0.1\%$   $P_2O_5$ ) [42]. These physical methods proved to be efficient to selectively separate ilmenite from monazite.

**Author Contributions:** C.C.G. performed all characterization analysis and mineral processing tests. P.F.A.B. contributed with the design of the mineral processing. Both C.C.G. and P.F.A.B. authors contributed to the final version of the manuscript. P.F.A.B. supervised the project.

**Funding:** This research received no external funding.

**Acknowledgments:** The authors acknowledge the Center for Mineral Technology (CETEM), which permitted this project development, and also the National Council for Scientific and Technological Development (CNPq) for the research grant; the Mineral Processing Laboratory of the University of São Paulo (LTM) for some tests, and the G-4 Esmeralda company for the PA sample.

**Conflicts of Interest:** The authors declare no conflict of interest.

## References

1. National Department of Mineral Production (DNPM). Sumário Mineral. c2010, c2011, c2012, c2013, c2014, c2015, c2016. Available online: <http://www.anm.gov.br/dnpm/publicacoes/serie-estatisticas-e-economia-mineral/sumario-mineral> (accessed on 15 November 2018).
2. Filho, P.C.S.; Serra, O.A. Terras raras no Brasil: Histórico, produção e perspectivas. *Química Nova* **2014**, *37*, 12.
3. Jones, G. *Mineral Sands: An Overview of the Industry*; Iluka Company: Perth, Australia, 2008; p. 26.
4. Gosen, B.S.V.; Bleiwas, D.I.; Bedinger, G.M.; Ellefsen, K.J.; Shah, A.K. Coastal deposits of heavy mineral sands: Global significance and US resources. *Min. Eng.* **2016**, *68*, 36–43.
5. Sampaio, J.A.; Luz, A.B.; Alcantera, R.M.; Araújo, L.S.L. *Minerais Pesados Millennium. Usinas de Beneficiamento de Minérios no Brasil*; Sampaio, J.A., Luz, A.B., Lins, F.F., Eds.; Center for Mineral Technology: Rio de Janeiro, Brazil, 2001; p. 233.
6. Schnellrath, J.; Monte, M.B.M.; Veras, A.; Júnior, H.R.; Figueiredo, C.M.V. *Minerais Pesados INB. Usinas de Beneficiamento de Minérios no Brasil*; Sampaio, J.A., Luz, A.B., Lins, F.F., Eds.; Center for Mineral Technology: Rio de Janeiro, Brazil, 2001; p. 189.
7. Rosental, S. *Terras Raras, Rochas e Minerais Industriais Usos e Especificações*; Luz, A.B., Lins, F.F., Eds.; Center for Mineral Technology: Rio de Janeiro, Brazil, 2005; p. 727.
8. Laxmi, T.; Srikant, S.S.; Rao, D.S.; Rao, R.B. Beneficiation studies on recovery and in-depth characterization of ilmenite from red sediments of badlands topography of Ganjam District, Odisha, India. *Int. J. Min. Sci. Technol.* **2013**, *23*, 725–731. [[CrossRef](#)]
9. Routray, S.; Rao, R.B. Beneficiation and Characterization of Detrital Zircons from Beach Sand and Red Sediments in India. *J. Miner. Mater. Charact. Eng.* **2011**, *10*, 1409–1428. [[CrossRef](#)]
10. Routray, S.; Laxmi, T.; Rao, R.B. Alternate Approaches to Recover Zinc Mineral Sand from Beach Alluvial Placer Deposits and Bandlands Topography for Industrial Applications. *Int. J. Mater. Mech. Eng.* **2013**, *2*, 80–90.
11. Tranvik, E.; Becker, M.; Palsson, B.I.; Franzidis, J.P.; Bradshaw, D. Towards cleaner production—Using floatation to recover monazite from a heavy mineral sands zircon waste stream. *Miner. Eng.* **2017**, *101*, 30–39. [[CrossRef](#)]
12. Moore, P. Heavy Minerals. *Int. Min.* **2011**, *1*, 7.
13. Worobiec, A.; Stefaniak, E.A.; Potgieter-Vermaak, S.; Sawłowicz, Z.; Spolnik, Z.; Grieken, R.V. Characterization of concentrates of heavy minerals sands by micro-Raman spectrometry and CC-SEM/EDX with HCA. *Appl. Geochem.* **2007**, *22*, 2078–2085. [[CrossRef](#)]
14. Mudd, G.M.; Jowitt, S.M. Rare earth elements from heavy mineral sands: Assessing the potential of a forgotten resource. *Appl. Earth Sci.* **2016**, *125*, 107–113. [[CrossRef](#)]
15. Silveira, F.V.; Chemale, L.T. *Minerais Estratégicos: Avaliação do Potencial de Terras Raras do Brasil*; Serviço Geológico do Brasil—CPRM: Brasília, Brazil, 2012; p. 38.
16. Chemale, L.T. *Avaliação do Potencial de Terras Raras do Brasil*; Serviço Geológico do Brasil—CPRM: Brasília, Brazil, 2013; p. 23.
17. Louwerse, D. Rare Earth Element Deposits and Occurrences within Brazil and India—Indicating and Describing the Main REE Deposits and Occurrences and Their Potentialities. Bachelor’s Thesis, Delft University of Technology, Delft, The Netherlands, 2016; p. 62.

18. Center for Mineral Technology (CETEM). *Exploração de Terras Raras em São Francisco do Itabapoana (RJ) Afeta Meio Ambiente, Banco de Dados de Recursos Minerais e Territórios: Impactos Humanos, Socioambientais e Econômicos*; Center for Mineral Technology: Rio de Janeiro, Brazil, 2013.
19. Krishnamurthy, N.; Gupta, C.K. *Extractive Metallurgy of Rare Earths Second Edition*; CRC Press: Boca Raton, FL, USA, 2016; p. 839.
20. Sabedot, S.; Sampaio, C.H. Caracterização de zircões da Mina Guaju (PB). *Revista Escola de Minas* **2002**, *55*, 5. [[CrossRef](#)]
21. Sabedot, S. Caracterização Tecnológica e Beneficiamento Mineral Para a Produção de Concentrado de Zircão de Alta Qualidade, Partindo de Pré-Concentrado e Concentrado de Zircão de Baixa Qualidade, Produzidos na Mina do Guaju (PB). Ph.D. Thesis, Universidade Federal do Rio Grande do Sul, Porto Alegre, Brazil, 2004; p. 114. (In Portuguese)
22. Ferreira, K.R.S. Caracterização do Concentrado de Ilmenita Produzido na Mina do Guaju, Paraíba, Visando Identificar Inclusões de Monazita e Outros Contaminantes. Master's Thesis, Universidade Federal do Rio Grande do Sul, Porto Alegre, Brazil, 2006; p. 64. (In Portuguese)
23. Ferreira, K.R.S.; Sabedot, S.; Sampaio, C.H. Evaluation of monazite presence in ilmenite concentrates produced at Guaju Mine (PB). *Revista Escola de Minas* **2007**, *60*, 669–673. [[CrossRef](#)]
24. Rio Grande Mineração. *Relatório de Impacto Ambiental Projeto Retiro*; CPEA—Consultoria, Planejamento e Estudos Ambientais Ltda and HAR Engenharia e Meio Ambiente Ltda: São José do Norte, Brazil, 2014; p. 37.
25. U.S. Geological Survey. *Mineral Commodity Summaries 2017*; U.S. Geological Survey: Reston, VA, USA; U.S. Department of Interior: Washington, DC, USA, 2017; p. 206.
26. Santos, J.F. *Technical Report 36: Titanium Profile*; J. Mendo Consultoria: Brasília, Brazil, 2010; p. 34.
27. Noguti, I.; Feitosa, J.A. *Potencial de Minerais Pesados na Região de Valença-Itacaré, Bahia—Amostragem, Caracterização e Tratamento do Minério*; Companhia Bahiana de Pesquisa Mineral: Salvador, Brazil, 1970; p. 18.
28. Andrade, A.C.S.; Dominguez, J.M.L. Informações geológico-geomorfológicas como subsídios à análise ambiental: Exemplo da planície costeira de Caravelas-Bahia. *Boletim Paranaense de Geociências* **2002**, *1*, 8. [[CrossRef](#)]
29. Brazilian Mineral Resources Company (CPRM). *Mapa geológico do estado do Piauí*; Serviço Geológico do Brasil: Brasília, Brazil, 2014; p. 1.
30. Moraes, A.M. *Diagnóstico e Diretrizes Para o Setor Mineral do Estado do Piauí—Parte I Caracterização Geral do Estado*; Ministério de Minas e Energia and Governo do Estado do Piauí: Teresina, Brazil, 2004; p. 170.
31. Mendes, J.C. Monazita e outros minerais pesados da região de Prado-Caravelas, no sul da Bahia. In Proceedings of the III Seminário Brasileiro de Terras Raras, Rio de Janeiro, Brazil, 27 November 2015; p. 14.
32. Cavalcanti, V.M.M. *Plataforma Continental: A Última Fronteira da Mineração Brasileira*; National Department of Mineral Production (DNPM): Brasília, Brazil, 2011; p. 96.
33. ICSD—Inorganic Crystal Structure Database. Available online: [https://http://www2.fiz-karlsruhe.de/icsd\\_home.html](https://http://www2.fiz-karlsruhe.de/icsd_home.html) (accessed on 14 December 2017).
34. Crystallography Open Database. Available online: <https://http://www.crystallography.net/cod/> (accessed on 14 December 2017).
35. Neumann, R.; Schneider, C.L.A.; Neto, A.A. *Caracterização Tecnológica de Minérios: Parte II. Tratamento de Minérios*; Luz, A.B., Sampaio, J.A., França, S.C.A., Eds.; Center for Mineral Technology: Rio de Janeiro, Brazil, 2010; p. 85.
36. Nair, A.G.; Babu, D.S.S.; Damodaran, K.T.; Prabhu, C.N. Weathering of ilmenite from Chavara deposit and its comparison with Manavalakurichi placer ilmenite, southwestern India. *J. Asian Earth Sci.* **2009**, *34*, 115–122. [[CrossRef](#)]
37. Weibel, R.; Friis, H. Alteration of opaque heavy minerals as a reflection of the geochemical conditions in depositional and diagenetic environments. *Dev. Sedimentol.* **2007**, *58*, 277–303.
38. Reyneke, L.; van der Westhuizen, W.G. Characterization of a heavy mineral-bearing sample from India and the relevance of intrinsic mineralogical features to mineral beneficiation. *Miner. Eng.* **2001**, *14*, 1589–1600. [[CrossRef](#)]
39. Dana, J.D. *Manual de Mineralogia*; Livros Técnicos e Científicos: Rio de Janeiro, Brazil, 1974; Volume 2, p. 287.
40. Temple, A.K. Alteration of ilmenite. *Econ. Geol.* **1966**, *61*, 695–714. [[CrossRef](#)]

41. Braccini, S.; Pellegrinelli, O.; Kramer, K. Mössbauer, X-Ray and magnetic studies of black sand from the Italian Mediterranean Sea. *World J. Nucl. Sci. Technol.* **2013**, *3*, 91–95. [[CrossRef](#)]
42. Cristal. Minérios. Available online: <https://www.cristal-al.com.br/nossos-produtos/minerios/> (accessed on 28 January 2019).



© 2019 by the authors. Licensee MDPI, Basel, Switzerland. This article is an open access article distributed under the terms and conditions of the Creative Commons Attribution (CC BY) license (<http://creativecommons.org/licenses/by/4.0/>).